Available online at www.sciencedirect.com

ScienceDirect

Underground Space 27 (2026) 321–339

www.keaipublishing.com/undsp

Research Paper

A perspective way for judging tunnel approach zones by cognitive-behavioral chains and predictive processing model

Runzhao Bei [a,b], Zijun Du [a,b,*], Nengchao Lyu [a,b], Zhigang Du [c]

[a] *Intelligent Transportation Systems Research Center, Wuhan University of Technology, Wuhan 430063, China*
[b] *Engineering Research Center of Transportation Information and Safety, Ministry of Education, Wuhan 430063, China*
[c] *School of Transportation and Logistics Engineering, Wuhan University of Technology, Wuhan 430063, China*

Received 30 August 2025; received in revised form 7 December 2025; accepted 25 December 2025
Available online 1 February 2026

Abstract

In tunnel approach zones (TAZs), drivers must complete a sequence of tasks, including detecting the tunnel, identifying speed limits, and decelerating to enter safely. However, current standards mandate only stopping sight distance (SSD) compliance of TAZs, which may not suffice for all of these complex driving tasks. In this study, we investigated (1) whether SSDs are sufficient for driving tasks in TAZs, (2) the impacts of restricted visibility conditions on cognitive-behavioral processes, and (3) the appropriate visibility condition of TAZs. We selected tunnels with three visibility conditions to conduct both subjective tests of perception and experiments with real vehicles. We propose a research framework called the task analysis of driving scenarios modified predictive processing model (TADS-MPPM). We then construct a multidimensional framework that includes sequences of behaviors and cognitive tasks (with 4 driving behavior nodes and 4 cognitive nodes) for spatiotemporal profiling, as well as active deceleration coefficients (safety and efficacy coefficients) and cognitive-behavioral workload (measured using the extended Jaccard coefficient). Then, we use an MPPM to visualize the evolution of driving predictions, driving behaviors, and sensory inputs during the approach to the tunnel. Finally, we explore the risk mechanisms of TAZs. The results show that SSD designs (1) delay tunnel detection, speed-limit recognition, and deceleration initiation, as well as compressing behavioral-cognitive chains, and (2) degrade safety and compliance due to overloaded operations and cognition. Conversely, ensuring that critical tunnel information is discernible at a longer decision sight distance provides the necessary margin of safety on the road. This creates adequate space and time to perform progressive deceleration to eliminate task compression and restore composed and smooth driving maneuvers.

Keywords: Road traffic safety; Tunnel approach zones; Driving behavior; Sight distance; Human factors

1 Introduction

Safety is still the most critical issue in the design of tunnels for human usage (Dou et al., 2023), and sight distance design is crucial for traffic safety (Feng et al., 2025; Hu et al., 2022) because an adequate sight distance provides drivers with sufficient perception–reaction time to complete driving tasks without an unsafe level of haste (Liu et al., 2025). When approaching a tunnel, drivers must perform a series of tasks such as recognizing the tunnel, identifying speed limits, and decelerating. This study defines tunnel approach zones (TAZs) as the upstream sections in which drivers' cognition or behavior is affected by the tunnel. However, current design standards, including China's JTG D20—2017 (Ministry of Transport of the People's Republic of China (MOT), 2017) and the US Green Book (American Association of State Highway and Transportation Officials (AASHTO), 2018), do not explicitly treat TAZs as complex driving environments in geometric, traffic safety facilities, or landscape design, and only require the stopping sight distance (SSD) to be

* Corresponding author at: Intelligent Transportation Systems Research Center, Wuhan University of Technology, Wuhan 430063, China.
E-mail address: duzj@whut.edu.cn (Z. Du).
Peer review under the responsibility of Tongji University

https://doi.org/10.1016/j.undsp.2025.12.002

satisfied. In fact, accident statistics show that accident rates and severity in the tunnel access zone (one SSD upstream of the tunnel portal) are not lower than those in the entrance zone (one SDS downstream of the tunnel portal) (Pervez et al., 2022; Wang et al., 2024; Yang et al., 2025), which is generally considered the most dangerous section inside the tunnel (Ju et al., 2025).

These findings indicate that driving in TAZs is both task-intensive and high-risk. Therefore, the following questions arise: Is SDS sufficient in TAZs? If not, how does an insufficient sight distance lead to high safety risks? What visibility conditions meet the safety requirements of TAZs? To answer these questions, it is necessary to quantify the cognitive-behavioral evolution process of TAZs and analyze the impact of different sight distances on this process. However, existing research has limitations. Although some evaluation indicators have been developed for the tunnel entrance area, they are only suitable for evaluative research and cannot support the exploration of the cognitive-behavioral evolution process (Bei et al., 2025).

We make three key contributions to fill these research gaps. First, we develop a model referred to as task analysis of driving scenarios and modified predictive processing model (TADS-MPPM) research framework to explore mechanisms of risk in TAZs. Second, we discover that merely meeting the SSD in TAZs does not guarantee driving safety and uncover the mechanism through which limited sight distance causes high safety risks. Third, we propose and empirically verify that ensuring the discernibility of the critical tunnel information (speed limit signs, tunnel information signs, and the portal) at the longer decision sight distance (DSD) provides the necessary safety margin for TAZ operations.

The remainder of this study is organized as follows. Section 2 reviews the sight-distance standards for TAZs and the limitations of current methods for exploring risk mechanisms in complex driving scenarios. Section 3 details the characteristics of the participants as well as the experimental setup, design, and the methods used to extract the dependent variable. Section 4 introduces the principle of constructing evaluation indicators based on TADS, and presents the results. Section 5 explores the risk mechanism of TAZs based on MPPM. Finally, Section 6 summarizes the main findings, acknowledges study limitations, and outlines directions for future research.

2 Literature review

2.1 Sight distance criteria in tunnel approach zones

To reduce structural risks and construction costs, tunnel designs often eliminate shoulders and substitute them with maintenance walkways. Although cost-effective, this compromises lateral safety buffers. In addition to inherently confined tunnel environments, restricted sightlines, and monotonous visual cues, safety risks are amplified (Ling et al., 2025; Xu et al., 2025a; Zhang et al., 2019). Mitigation strategies such as reduced speed limits and lane-change prohibitions are typically implemented within tunnels. Crucially, however, drivers encounter abrupt transitions at tunnel portals (Bei et al., 2025; Du et al., 2014; Han & Du, 2025; Xu et al., 2025b; Yang et al., 2024), road cross-sections, longitudinal visual references, illumination (sudden luminance changes), and speed regulation shift dramatically. These disruptions impair the longitudinal speed control (Ju et al., 2025b) and lateral positioning (Bei et al., 2024) of the drivers.

Consequently, for a safe and smooth transition from open roads into tunnels, drivers require sufficient upstream distance to (1) clearly identify the tunnel, (2) detect and comprehend speed limit signs, and (3) initiate necessary deceleration. This underscores that tunnel safety requires integrating the critical upstream transition zone.

Current tunnel safety practices (e.g., lighting design) and accident analysis (Amundsen & Ranes, 2000; Ma et al., 2016) typically consider only an SSD upstream—a distance based on reaction and braking mechanics. However, studies have shown that tunnels influence driver cognition and behavior far upstream, well beyond the SSD (Bei et al., 2025). While many accidents occur near the portal or within one SSD upstream (Amundsen & Ranes, 2000; Pervez et al., 2020), they may stem from accumulated cognitive-behavioral errors upstream (e.g., delayed portal detection, slow response to speed signs, and inadequate/deceleration), culminating at the high-risk portal areas (Bei et al., 2025). Truly effective accident prevention requires greater spatial margins upstream (He et al., 2025), allowing adequate time and distance for the complex perception–cog nition–decision–action process before encountering portal risks.

Thus, we propose studying upstream tunnel zones that specifically focus on driver cognition and behavior. We formally define TAZs as the upstream area in which the cognitive-behavioral processes of the drivers are significantly altered by the approaching tunnel. Defining TAZs is fundamental for investigating upstream risk mechanisms and developing targeted countermeasures.

Current standards only mandate SSD within TAZs (JTG D20—2017 and the US Green Book). The SSD represents the minimum distance to brake after detecting a stationary obstacle, considering collision avoidance alone (Feng et al., 2025; Hu et al., 2022). In contrast, DSD provides the distance needed for the full perception–cognition–decision sequence in complex scenarios (e.g., identifying signs, assessing risks, and executing maneuvers such as lane changes or controlled deceleration) (AASHTO, 2018), significantly exceeding the SSD and providing a crucial safety margin. Therefore, we recommend adopting DSD as the sight distance standard for TAZs. Drivers must clearly see critical tunnel-related information (e.g., speed limit signs, tunnel information boards, and the portal itself) from at least one DSD upstream of the portal.

2.2 Limitations of current evaluation index systems

Regarding tunnel entrance areas, the logic of constructing the evaluation index system in existing research can be summarized as follows. First, the behavior of the entire driving group is represented as the behavior of a single sample driver (Calvi et al., 2012; Fang et al., 2022; Hu et al., 2016; Yan et al., 2022; Zhang et al., 2023) (Method 1). Alternatively, statistical analysis can be conducted by considering the tunnel entrance area as a whole (Hu et al., 2019; Shao et al., 2022; Wang et al., 2016; Zhu et al., 2020) (Method 2). The tunnel entrance area can be further subdivided into different functional zones (such as access, entrance, and transition) (Han et al., 2024a; He et al., 2017; Shao et al., 2022; Yan et al., 2022) or sections with equal-distance intervals (such as increments of 20–50 m) (Fang et al., 2022; Han et al., 2024b; Hu et al., 2019; Liu et al., 2011; Wang et al., 2016b), and then conduct independent statistical analysis in each sub-zone (Method 3).

However, when analyzing the risk mechanisms of complex driving scenarios, the abovementioned logic of constructing an index system involves some obvious limitations. Firstly, Method 1 relies on a single-sample representation, which results in the loss of a large amount of heterogeneous information about the driving group and fails to reflect the group behavior patterns. Secondly, Method 2 uses full-scale statistics, which mask the dynamic changes and differences in driving behaviors in different subsections within the tunnel entrance area. Finally, although Method 3 can reflect the macroscopic differences in sub-areas through zoning, it fails to solve a key problem: within the same divided sub-zone, drivers may be in different stages of behavioral evolution. Mixing driving data from different behavioral stages for statistical analysis in the same zone will lead to mutual interference of information between stages, thus diluting the change signals of behavioral characteristics.

Therefore, the existing methods for constructing an evaluation index system are primarily applicable to macroscopic evaluation research and largely lack the capability to support the analysis of the fine evolution mechanism of cognitive behavior while driving. To address this gap, we leverage TADS to develop a refined evaluation index system as described in Sections 3 and 4.

2.3 Lack of frameworks for explaining risk mechanisms

Sight distance fundamentally shapes the sensory inputs, expectations, and behaviors of the drivers, which collectively determine task performance (Bei et al., 2025). In complex driving scenarios, expectations and behaviors evolve dynamically as drivers interact with rapidly changing environments. The phased evolution of driving expectations serves as a critical mediator between environmental stimuli and behavioral outputs, and accurate predictive processing enables drivers to anticipate evolving roadway demands and execute timely maneuvers (Koustanaï et al., 2008; Muhrer & Vollrath, 2010). Quantifying the interplay among tasks, expectations, and behavior is essential to identifying latent risk mechanisms.

However, a unified model that integrates these elements is lacking, which limits mechanistic exploration. Traditional frameworks acknowledge driver anticipation but often treat cognitive processes opaquely (Wickens, 2008). Dominant models, such as the perception–reaction model, conceptualize behavior linearly through stimulus–response patterns. For example, Bei et al. (2024) measured intervals between tunnel speed-limit sign fixation and deceleration onset, while Wang et al. (2016a) calculated response times from lead-vehicle braking to throttle release. Although useful for empirical risk assessment, these temporal metrics primarily quantify observable behavioral outputs rather than elucidating the hierarchical cognitive mechanisms governing anticipation.

The predictive processing model (PPM) (Bei et al., 2025) overcomes this limitation by modeling cognition and behavior as a process of active inference, in which drivers continuously minimize prediction errors through hierarchical feedback loops between sensory input and contextual expectations. To advance this framework in TAZs, we propose the MPPM. Integrated with our evaluation system, the MPPM is used to visualize the spatiotemporal evolution of driving predictions, behaviors, and sensory inputs to reveal the risk mechanisms (detailed in Section 5).

3 Methodology

3.1 Apparatus and participants

We equipped an instrumented sedan with a multi-sensor array comprising (1) a stereo camera (Smarter Eye), (2) an onboard diagnostics system (OBD-II), (3) a dashcam (DDPAI MIMI5), and (4) an eye-tracking device (Dikablis Glasses 3). This configuration recorded four key data types, including vehicle kinematic data (e.g., velocity and lateral deviation), vehicle operational data (e.g., throttle position), forward roadway video, and driver eye movement behavior. This instrumentation setup is shown in Fig. 1.

A total of 33 licensed drivers were initially recruited. A pre-experiment involving three of these individuals (2 males, 1 female) was conducted to validate the feasibility of the experimental procedure and the performance of the equipment. The remaining 30 participants proceeded to the formal experiment. Consequently, the final valid sample comprised 30 participants. This sample size is greater than that of comparable experimental driving studies (Han et al., 2024; Ju et al., 2025a). All participants in the final sample reported having normal or corrected-to-normal vision, confirmed no prior familiarity with the experimental routes, and stated that they were well-rested

Fig. 1. Test apparatus.

Table 1
Demographic profile of the final participant sample ($n = 30$).

Characteristic	Description
Gender	20 males (66.7%), 10 females (33.3%)
Age (y)	M = 38.5, SD = 9.6, Range: 22–60
Age distribution	22–25 y: 20.0% ($n = 6$)
	26–50 y: 66.7% ($n = 20$)
	51–60 y: 13.3% ($n = 4$)
Driving experience (y)	M = 10.3, SD = 6.9, Minimum: 3

Note: M = Mean; SD = Standard Deviation. This sample was selected to represent the gender and age structure of China's driver population.

and fit to drive prior to each testing session. The key demographic characteristics of the final participant group are summarized in Table 1.

3.2 Scenarios

Given the significant influence of the characteristics of the roadway, tunnel, and signage on the behavior of drivers, these elements are first described below to establish the necessary context before explaining the independent variable and the control of confounding factors in detail.

3.2.1 Characteristics of test route, tunnels, and signage

The test route was located on a bidirectional six-lane freeway in Guangdong, China. The roadway has a lane width of 3.75 m and a design speed of 120 km/h outside tunnels. The width of the right hard shoulder is 3.00 m. Inside tunnels, the speed limits are set at 80 km/h for buses and trucks and 100 km/h for cars, with a maintenance walkway width of 0.75 m and left/right lateral clearances (L_L and L_R) of 0.75 and 1.00 m, respectively.

The route includes 18 tunnels. Since the TAZs are the focal sections of this study and form the basis for controlling confounding variables, their horizontal and vertical alignments are summarized in Table 2. Existing research indicates that the radius and deflection of curves, as well as gradient, are the primary geometric elements influencing driving behavior (Bei et al., 2025; Han & Du, 2025). Therefore, Table 2 presents these parameters. All TAZs satisfy the SSD requirement.

The tunnels and their approach zones follow uniform design standards, as shown in Fig. 2. Each tunnel has an interior cross-section of 14.5 m in width and 7 m in height. Externally, the first 80 m of the approach zone features solid lane lines supplemented by longitudinal speed-reduction markings, followed by three sets of transverse rumble strips between 80 and 160 m from the portal. A 12-m guardrail transition section is installed on the right side. The approach zone includes placed speed limit, no-lane-change, and tunnel information signs, with their specific layout detailed in Fig. 2(c). All design parameters comply with JTG/T D70/2–02—2014 and GB 5768.3—2025 (MOT, 2014, 2025).

Table 2
Geometric alignment characteristics of all TAZs along the test route.

Serial number of TAZs	Radius of curve (m)	Deflection	Gradients (%)
1-East	2000	Right	−0.50
1-West	2000	Left	+0.50
2-East	2350	Left	−0.38
2-West	0	Straight	+0.38
3-East	0	Straight	−1.65
3-West	2000	Left	+1.65
4-East	1600	Left	−1.85
4-West	1600	Right	+1.85
5-East	0	Straight	+0.60
5-West	5500	Left	+2.00
6-East	0	Straight	+0.55
6-West	0	Left	+2.18
7-East	3300	Left	−1.59
7-West	1700	Left	+1.59
8-East	0	Straight	+0.60
8-West	1800	Left	+1.60
9-East	0	Straight	−0.96
9-West	1750	Left	+0.96

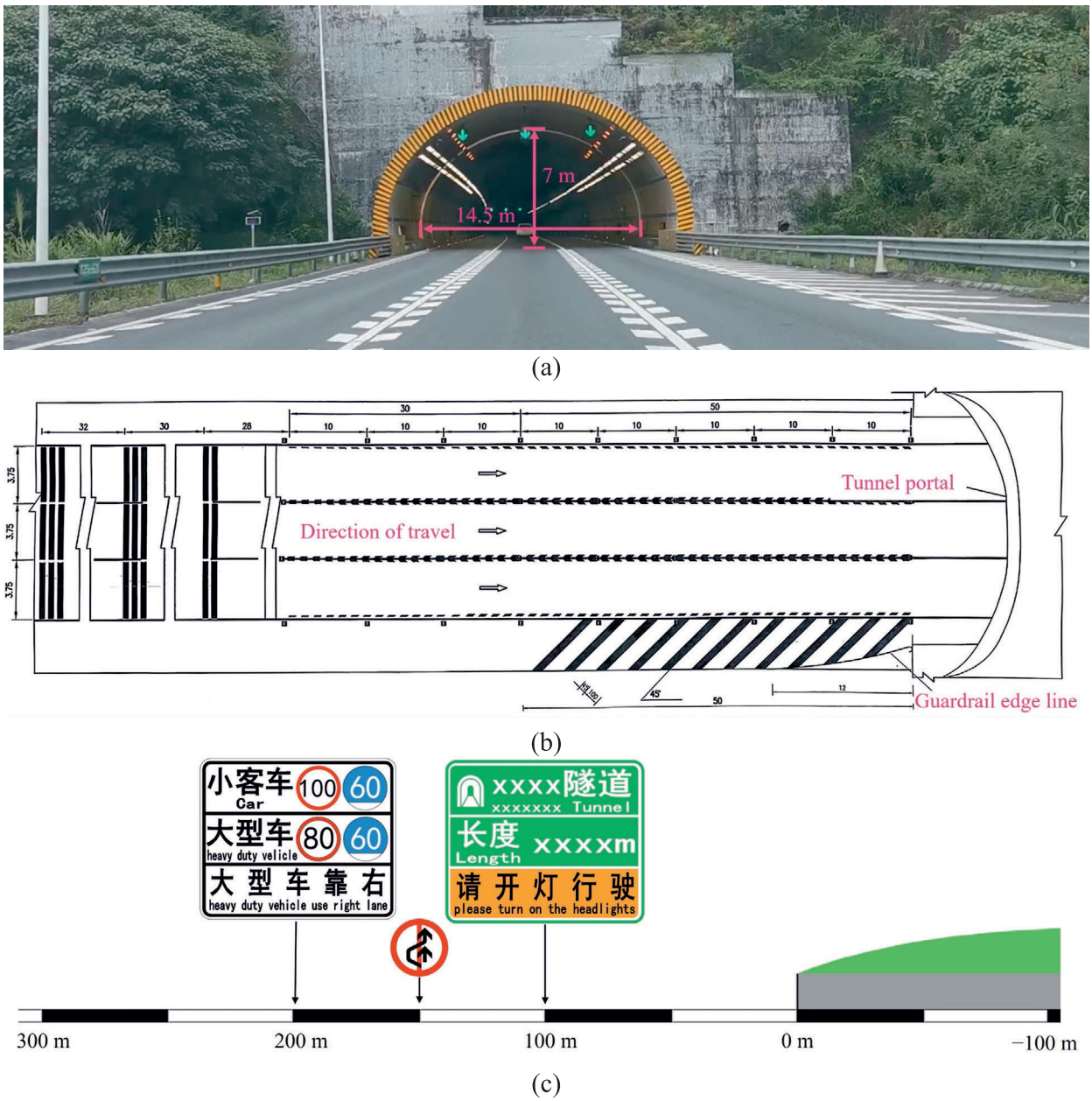

Fig. 2. Configuration details of tunnel portals and approach zone traffic control devices. (a) Cross-sectional tunnel dimensions, (b) pavement markings and guardrail transition, and (c) layout of regulatory and informational signs.

3.2.2 Independent variable and control of confounding factors

Given the high cognitive and operational requirements of TAZs, we argue that visibility conditions should allow drivers to spot an approaching tunnel at a distance equal to the DSD. Thus, the visibility conditions of TAZs were designated as the independent variable to investigate their influence on driving behavior and cognition. As tunnel detection primarily relies on key visual cues—specifically, speed limit signs, tunnel information signs, and the portal itself—this variable was classified into three discrete levels based on the detectability of these critical elements at a distance of one DSD from the tunnel portal, as illustrated in Fig. 3.

(1) Visible: All critical information elements are fully discernible at the DSD location. This represents the recommended visibility conditions for TAZs.
(2) Partially visible: Only a subset of critical information is detectable at the DSD location. This complies only with SSD requirements.
(3) Not visible: No critical information elements are detectable at the DSD location. As with the previous condition, it complies only with the SSD requirement.

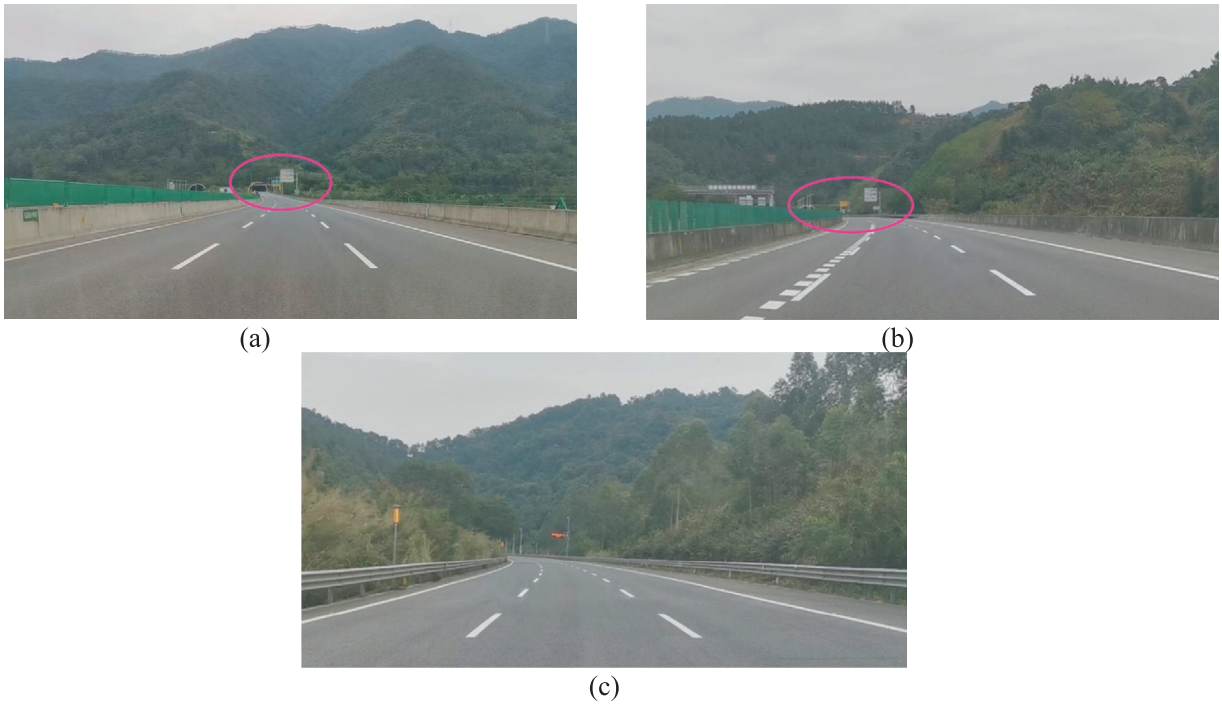

Fig. 3. Visibility conditions of tunnel approach zones. (a) 3-West: visible, (b) 8-West: partially visible, and (c) 4-East: not visible.

To isolate the effect of TAZs visibility conditions, confounding variables were rigorously controlled through the following principles: (1) upstream tunnel separation: the distance to the preceding tunnel exit >1500 m (minimizing operational interference from adjacent tunnels); (2) grade severity limitation: absolute longitudinal slope magnitude ≤3% (Wang et al., 2023); (3) horizontal curvature constraint: the radius of the horizontal curve maintained between 1500 and 2000 m; (4) alignment direction consistency: uniform direction of approach zone curves across selected sites.

Based on these stringent criteria, three eligible tunnels were identified from the initial 18-tunnel inventory. Their detailed geometric parameters and classified visibility conditions are presented in Table 3. The SSD and DSD values correspond to a design speed of 120 km/h, with SSD of 250 m and DSD of 415 m (Condition D per the US Green Book, which reflects the complexity of freeway tasks and the characteristics of traffic).

3.3 Preliminary experiment and task analysis of driving scenarios

A pre-experiment involving three participants (2 males, 1 female) was conducted prior to the main study. Its objectives were to (1) validate the feasibility of the experimental procedure and the performance of the data acquisition equipment, (2) preliminarily explore driving behaviors within highway tunnel approach zones, and (3) inform the design of the subsequent subjective perception experiment. These participants did not take part in the formal experiment. The specific procedure for the pre-experiment, which was conducted using a real vehicle, is described in detail in Section 3.4 (formal experiment).

Based on the data collected from this preliminary experiment, we applied the TADS framework to investigate driver anticipation and behavioral patterns in TAZs. This analysis postulates a conceptual relationship among the driving task requirements, the anticipatory cognitive

Table 3
Configuration and visibility of TAZs.

Tunnels	Distance to the previous tunnel (m)	Radius of curve (m)	Deflection	Longitudinal slope	Shelters	Recognition effects at DSD
3-West	3791.5	2000	Left	+1.65%	Nothing	Visible
8-West	1585	1800	Left	+1.60%	Left glare shield	Partially visible
4-East	3516	1600	Left	−1.85%	Trees on the left side and the mountain on the right side	Not visible

processes of the drivers, and their resulting observable behaviors within TAZs. The framework proposes that drivers' behavior transitions through distinct, sequential phases in a TAZ. An illustration of these phases, derived from data collected at Tunnel 3-West, is presented in Fig. 4.

The task zones of TAZs are defined as follows. This part only defines these concepts, and detailed data to support this categorization are provided in Section 4.

(1) Recognition zone: The first part of the approach zone is the recognition zone. When the driver is far from the tunnel, they cannot yet see tunnel-related signs or the portal. However, they can anticipate a tunnel ahead by observing environmental changes. Around this point, the vehicle starts to slow down gradually. These actions show that the driver is influenced by the upcoming tunnel and enters the approach zone. Then, they need more information to recognize the tunnel.
(2) Preparatory zone: Once the driver has gathered enough information (this can be measured by fixation behavior as they acquire information through gazing), they know they are approaching the tunnel. At this point, the vehicle enters the preparatory zone and starts getting ready to slow down.
(3) Deceleration zone: After recognizing the speed limit (also measurable by fixation behavior), the driver decides to decelerate and start the process.

3.4 Formal experiment

The formal experiment consisted of two sequential phases, including an experiment with a real vehicle to collect objective behavior, eye-movement, and video data, followed by a subjective perception experiment to retrospectively identify the locations where specific driving predictions were formed.

3.4.1 Real vehicle experiment

The experiment with the real vehicle was conducted on a closed-loop freeway circuit. The route originated at the service area directly upstream of Tunnel 1-East (between stake marks K178+059 and K177+544) and concluded at the service area downstream of Tunnel 1-West (between stake marks K177+529 and K178+064). Directional reversal was performed at the interchange downstream of Tunnel 9-East (between stake marks K289+098 and K288+552) to ensure that the circuit encompassed all 18 tunnels along the corridor. Participants were instructed to drive in the middle lane throughout the test to avoid the influence of guardrails and sidewalls near the left lane, which were not the focus of this study. Since one objective of this study was to examine the natural speed selection tendencies of the drivers, no specific speed was imposed beyond the posted limits. The drivers were free to choose their speed based on roadway environmental cues and the regulatory speed requirements. All experiments were conducted under free-flow traffic conditions to minimize the influence of surrounding vehicles. To ensure consistent visibility conditions, all test runs were scheduled during periods of stable, moderate sunlight: 8:00–11:00 AM and 2:00–5:00 PM. This control minimized the potential effects of glare or low illumination on the perception and behavior of the drivers.

The procedure for each test run was standardized as follows.

(1) Preparation: At the starting service area, the participants donned reflective safety vests. An eye-tracker was fitted and calibrated using a four-point calibration procedure. All other data acquisition systems (OBD-II, cameras) were verified for operational status.
(2) Driving: The participants received a brief overview of the test route. During the drive, the experimenters remained silent to avoid distraction. A dedicated test administrator recorded the overall start/end times and the precise timestamps of each tunnel entry and exit.
(3) Post-drive interview: Immediately after each run, a semi-structured interview was conducted to gather qualitative insights into the cognitive processes of the drivers related to tunnel detection and deceleration decision-making. The interview guide focused on the following key questions. Q1: What information did you pay the most attention to when approaching the tunnel? Q2: Before encountering

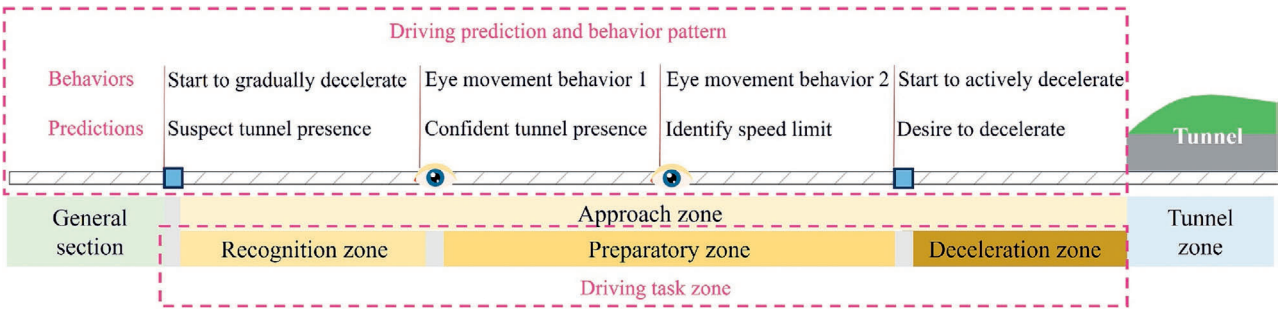

Fig. 4. Division of task zones and prediction–behavior patterns in TAZs.

the tunnel information sign, speed limit sign, or tunnel portal, were you aware that a tunnel lay ahead? If so, how was this awareness/detection achieved? Q3: At what specific point did you confirm the existence of the tunnel? What information confirmed its presence? Q4: At what moment (or based on what cue/situation) did you decide to initiate deceleration (start braking or lifting the accelerator)?

3.4.2 Subjective perception experiment

Based on the TADS conducted in the preliminary experiment, we analyzed the evolution of driver predictions upstream of Tunnel 3-West (visible), as illustrated in Fig. 4. This analysis suggested a sequential cognitive process in which the driver first suspects that a tunnel is coming up ahead, then confirms that there is one, identifies the speed limit, and decelerates appropriately. Following the formal experiment with a real vehicle, we analyzed the post-drive interview data to verify this hypothesized process with a richer dataset and to investigate whether different visibility conditions in the approach zone alter the evolution of driver predictions.

The analysis confirmed that the prediction sequence upstream of Tunnel 3-West (visible) consistently followed the pattern shown in Fig. 4. However, for Tunnel 8-West (partially visible) and Tunnel 4-East (not visible), the initial stage of suspecting the presence of the tunnel was absent. Under these restricted visibility conditions, the drivers only became aware of the tunnel at a short distance, and progressed rapidly through the subsequent stages of confirming tunnel presence while identifying the speed limit and desiring to decelerate. A detailed analysis of this conclusion is available in our dedicated study (Bei et al., 2025).

To spatially quantify the locations where these specific driving predictions were formed, we conducted a subjective perception experiment after the real-vehicle tests. First, we extracted 1500-m video segments upstream of the three tunnels (with different visibility conditions) for all participants using guardrail stake marks for precise truncation. These videos were then replayed to the participants, who were instructed to mentally simulate driving. They pressed the spacebar the moment they re-experienced each specific prediction. A custom-developed plugin automatically captured the corresponding video frame. The spatial location of the vehicle at that moment was then manually calculated based on the roadside stake marks and the speed of the vehicles.

Due to the identified differences in prediction evolution across visibility conditions, the tasks in the subjective experiment were tailored accordingly. For Tunnel 3-West (visible), the participants marked four prediction points, including (1) suspecting tunnel existence (becoming vaguely aware of a possible tunnel ahead based on contextual environmental changes, without certainty); (2) confirming tunnel existence (becoming certain of the tunnel's presence based on direct cues, e.g., tunnel information sign, speed limit sign, and portal); (3) clarifying the speed limit (seeing and comprehending the posted speed limit); (4) desire to decelerate: forming the intention to reduce speed. For Tunnels 8-West (partially visible) and 4-East (not visible), participants marked only three points, corresponding to stages (2), (3), and (4) above, as the initial suspicion stage was consistently absent.

4 Results

4.1 Cognitive-behavioral chain characteristics in TAZs

4.1.1 Indicators about cognitive-behavioral chain development

To quantitatively characterize the chains of driving behavior and cognition during tunnel approaches, we developed a series of evaluation metrics based on patterns of cognition during driving behavior derived from a TADS. These metrics were designed to capture (1) the key driving behavior nodes defined by objective vehicle control or eye-movement events, (2) the key cognitive nodes derived from subjective reporting, and (3) the safety and effectiveness of active deceleration behaviors, which were quantified by two novel coefficients. The complete indicator system is presented in Table 4 and the operational definitions of critical metrics are elaborated below.

Key driving behavior nodes and coefficients for active deceleration behavior were identified based on the time-series data of vehicle kinematics and driver eye movements. The specific detection methods are as follows.

(1) Objective position at which the driver starts to gradually decelerate (P_{OPSGD}): The throttle-opening position was normalized to a 0–100% scale, with 0% indicating that it was fully released and 100% indicating fully depressed. The onset of deceleration corresponds to the release of the throttle. P_{OPSGD} was identified by detecting a gentle throttle release, defined as the first location where the throttle opening begins to decrease, and the absolute rate of change in the throttle opening remains below 50%/s (Bei et al., 2024). This detection was further validated by a concurrent, sustained decline in vehicle speed.
(2) Objective position of ergodic fixation (P_{OPEF}): Drivers acquire information through visual fixations to form driving expectations, with a minimum duration of ≥100 ms typically required for effective information intake (Han et al., 2024). To accurately capture the completion of tunnel recognition, we defined the speed limit sign, tunnel information sign, and tunnel portal as areas of interest (AOIs). P_{OPEF} was determined as the vehicle position at which the driver fixated (≥100 ms) on all three critical tunnel-related AOIs. This definition followed from our comparative analysis, which showed that the position corresponding to the complete scan of all three elements best matched the subjective reported location of tunnel

Table 4
Evaluation indicator system for behavioral and cognitive chains.

Indicators		Meaning
Key driving behavior nodes	Objective position of starting to gradually decelerate, P_{OPSGD} (m)	Under the visible condition, vehicle speed begins to decrease gently at a considerable distance upstream, influenced by the approaching tunnel. This onset location (P_{OPSGD}) is identified by a subtle change in throttle opening position (<50% per second).
	Objective position of ergodic fixation, P_{OPEF} (m)	Based on driver interviews (Q3), tunnel presence is confirmed upon recognizing key elements: the speed limit sign, tunnel information sign, and the tunnel portal. We posit that a brief fixation (≥100 ms) on any of these elements signifies their conscious perception, thereby marking the location of tunnel confirmation as P_{OPEF}.
	Objective position of first fixation, P_{OPFF} (m)	To comprehend the posted speed limit, drivers require a prolonged fixation on the speed limit sign. We define the location of the first fixation lasting ≥300 ms on this sign as P_{OPFF}, indicating the position at which the speed limit requirement is understood.
	Objective position of starting to actively decelerate, P_{OPSAD} (m)	To comply with the tunnel speed limit, drivers execute an active deceleration maneuver before entry. The onset of this decisive action (P_{OPSAD}) is identified by a pronounced, rapid change in throttle opening position (≥50%/s).
Key cognitive nodes	Subjective position of suspecting tunnel presence, P_{SPSTP} (m)	P_{SPSTP} is the location where the driver first becomes vaguely aware of a possible tunnel ahead based on contextual environmental changes, without certainty.
	Subjective position of confirming tunnel presence, P_{SPCTP} (m)	P_{SPCTP} is the location where the driver becomes certain of the tunnel's presence based on direct visual cues (e.g., tunnel information sign, speed limit sign, and portal).
	Subjective position of identifying speed limit, P_{SPISL} (m)	P_{SPISL} is the location where the driver clarifies the speed limit requirement for the upcoming tunnel.
	Subjective position of desiring to decelerate, P_{SPDD} (m)	P_{SPDD} is the location where the driver forms the intention to actively decelerate.
Active deceleration behavior coefficients	Coefficient of active deceleration security, C_{ADS}	A safety index is calculated from the deceleration distance, the speed during deceleration, and the speed difference before and after deceleration. A higher value indicates a safer deceleration maneuver.
	Coefficient of active deceleration effect, C_{ADE}	Evaluate the compliance performance of the deceleration behavior based on the consistency between the speed at the tunnel portal and the regulatory speed limit. A higher value (max 1.0) indicates better compliance, with lower values reflecting greater severity of speed limit violation.

confirmation, typically following a sequential pattern (tunnel information sign → speed limit sign → portal). Fixations were detected using a D-Lab eye-tracking platform with a duration threshold of 100 ms.

(3) Objective position of first fixation (P_{OPFF}): P_{OPFF} was defined as the vehicle location at which the driver's first fixation on the speed limit sign reached or exceeded 300 ms. This threshold was selected after systematically testing several candidate durations (100, 200, and 300 ms). The 300 ms criterion yielded the closest spatial agreement with the subjectively reported position of speed limit comprehension, likely because the speed limit sign contains three distinct pieces of information that require integration for full understanding. Fixations were detected using the eye-tracking platform (D-Lab) with the selected 300 ms threshold applied during data extraction.

(4) Objective position at which the driver starts to actively decelerate (P_{OPSAD}): The detection method for P_{OPSAD} is analogous to that used for P_{OPEF} but distinguishes between gradual and active deceleration. P_{OPSAD} is identified by detecting a pronounced throttle release, defined as the first location where the throttle opening decreases, and the absolute rate of change in the throttle opening exceeds 50%/s (Bei et al., 2024). This higher threshold captures the onset of an active compliance-driven deceleration maneuver.

(5) Coefficient of active deceleration security (C_{ADS}): This coefficient was calculated using Eqs. (1) and (2) (Bei et al., 2025). Its formulation considers that a longer deceleration distance (X(m)), a smaller speed reduction (($V_1 - V_2$) m/s), and a lower speed (($V_1 + V_2$) m/s) during deceleration collectively contribute to a safer active deceleration behavior.

$$C_{ADS_{ij}} = \frac{X_{ij}}{(V_{1_{ij}} - V_{2_{ij}})(V_{1_{ij}} + V_{2_{ij}})} = \frac{X_{ij}}{V_{1_{ij}}^2 - V_{2_{ij}}^2}, \tag{1}$$

$$C_{ADS_j} = \sum_{i=1}^{30} C_{ADS_{ij}}/30, \tag{2}$$

where i represents the ith participant, j is the jth scenario, X is the length of the active deceleration segment (distance from P_{OPSAD} to the tunnel portal), V_1 is the speed at P_{OPSAD}, and V_2 is the speed at the tunnel entrance.

(6) Coefficient of active deceleration effect (C_{ADE}): This coefficient was calculated using Eqs. (3)–(5) (Bei et al., 2025). It relates the tunnel's speed limit (100 km/h) to the vehicle speed at the portal (V_2).

$C_{ADE} = 1$ indicates that V_2 is at or below the limit. When V_2 exceeds the limit, the value decreases proportionally with the magnitude of the violation, reflecting poorer deceleration effectiveness.

$$M = \max\{V_{2_{ij}}\} - 100, \tag{3}$$

$$C_{ADE_{ij}} = \begin{cases} 1 - (V_{2_{ij}} - 100)/M & , V_{2_{ij}} > 100 \\ 1 & , V_{2_{ij}} \le 100 \end{cases}, \tag{4}$$

$$C_{ADE_j} = \sum_{i=1}^{30} C_{ADE_{ij}}/30, \tag{5}$$

where the sequence $\{V_{2ij}\}$ encompasses all the recorded V_2 values from the experiment.

4.1.2 Statistical analysis of cognitive-behavioral chain indicators

Table 5 presents means, standard deviations (in parentheses), and one-way ANOVA results (F) for behavioral and cognitive evolution metrics. All distances are reported relative to the tunnel portal (0 m), with positive values indicating upstream locations. The "NA" in the ANOVA column indicates that statistical testing was not applicable, not a lack of difference. This applies to two cases: (1) P_{OPSGD} and P_{SPSTP}, which were only observed under the visible condition; (2) the aggregated coefficients C_{ADS} and C_{ADE}, which are scenario-level metrics unsuitable for ANOVA. Crucially, all other comparable metrics showed statistically significant differences ($p < 0.001$) across visibility conditions. This confirms that SSD-compliant designs (partial and not visible) significantly impair driver cognition and behavior compared to the DSD-compliant (visible) benchmark. The descriptive decline in C_{ADS} and C_{ADE} values further supports this safety compromise.

Figure 5(a)–(d) compares the distributions of key behavior and cognition nodes under different visibility conditions using violin plots. One-way ANOVA (left annotations) and LSD post-hoc tests (plot annotations) assess significance (NS for $p \ge 0.05$, * for $p \le 0.05$, ** for $p \le 0.01$, *** for $p \le 0.001$, and **** for $p \le 0.0001$). Figure 5(e)–(f) further illustrates the safety and effectiveness of active deceleration under varying visibility conditions.

Key findings from Fig. 5 and Table 5 are as follows:

(1) Under DSD-compliant (visible) conditions, drivers exhibited early adjustments.

Gradual deceleration (P_{OPSGD}) began at 830.01 m, even before conscious suspicion of the tunnel (P_{SPSTP}) was reported at 804.59 m. This anticipatory behavior expands the available space and time for subsequent tasks. In contrast, SSD-compliant designs (partially or not visible) eliminate this early phase, compressing the entire cognitive-behavioral chain closer to the portal.

(2) The objective eye movement metrics strongly corresponded to the subjective cognitive reports.

No significant difference was found between P_{SPCTP} and P_{OPEF} across visibility levels, validating that a fixation (≥100 ms) on tunnel related elements signals the drivers' detection and corresponding expectation of the tunnel ahead. Similarly, P_{SPISL} and P_{OPFF} were statistically equivalent, confirming that a longer fixation (≥300 ms) on the speed limit sign reflects comprehension of the speed limit.

(3) SSD compliance induced substantial and graded cognitive delays.

Compared with the baseline visible condition ($P_{OPEF} =$ 454.72 m, $P_{OPFF} =$ 364.01 m), tunnel detection shifted 33.8% closer to the portal under partially visible conditions and 47.0% closer under not visible conditions. The speed limit recognition was delayed by 21.4% and 30.1%, respectively. This demonstrates SSD's inadequacy of SSD in providing sufficient time for task execution in the TAZs.

Table 5
Statistical analysis of indicators for behavioral and cognitive evolution.

Indicators		Visibility of tunnel approach zones			F	p
		Visible	Partially visible	Not visible		
Key driving behavior nodes	P_{OPSGD} (m)	830.01(30.61)	NA	NA	NA	NA
	P_{OPEF} (m)	454.72(21.45)	301.26(23.92)	241.22(13.72)	893.79	0.000*
	P_{OPFF} (m)	364.01(18.69)	286.05(25.12)	254.61(13.45)	245.89	0.000*
	P_{OPSAD} (m)	306.54(18.25)	254.66(25.33)	231.22(12.89)	117.2	0.000*
Key cognitive nodes	P_{SPSTP} (m)	804.59(35.22)	NA	NA	NA	NA
	P_{SPCTP} (m)	450.55(22.65)	300.42(25.24)	240.43(15.62)	756.35	0.000*
	P_{SPISL} (m)	362.26(20.97)	284.18(26.83)	253.78(16.32)	197.65	0.000*
	P_{SPDD} (m)	329.54(19.10)	271.00(26.71)	240.28(13.48)	146.92	0.000*
Active deceleration behavior coefficients	C_{ADS}	0.76	0.58	0.51	NA	NA
	C_{ADE}	0.95	0.83	0.81	NA	NA

* Indicates that $p \le 0.05$.

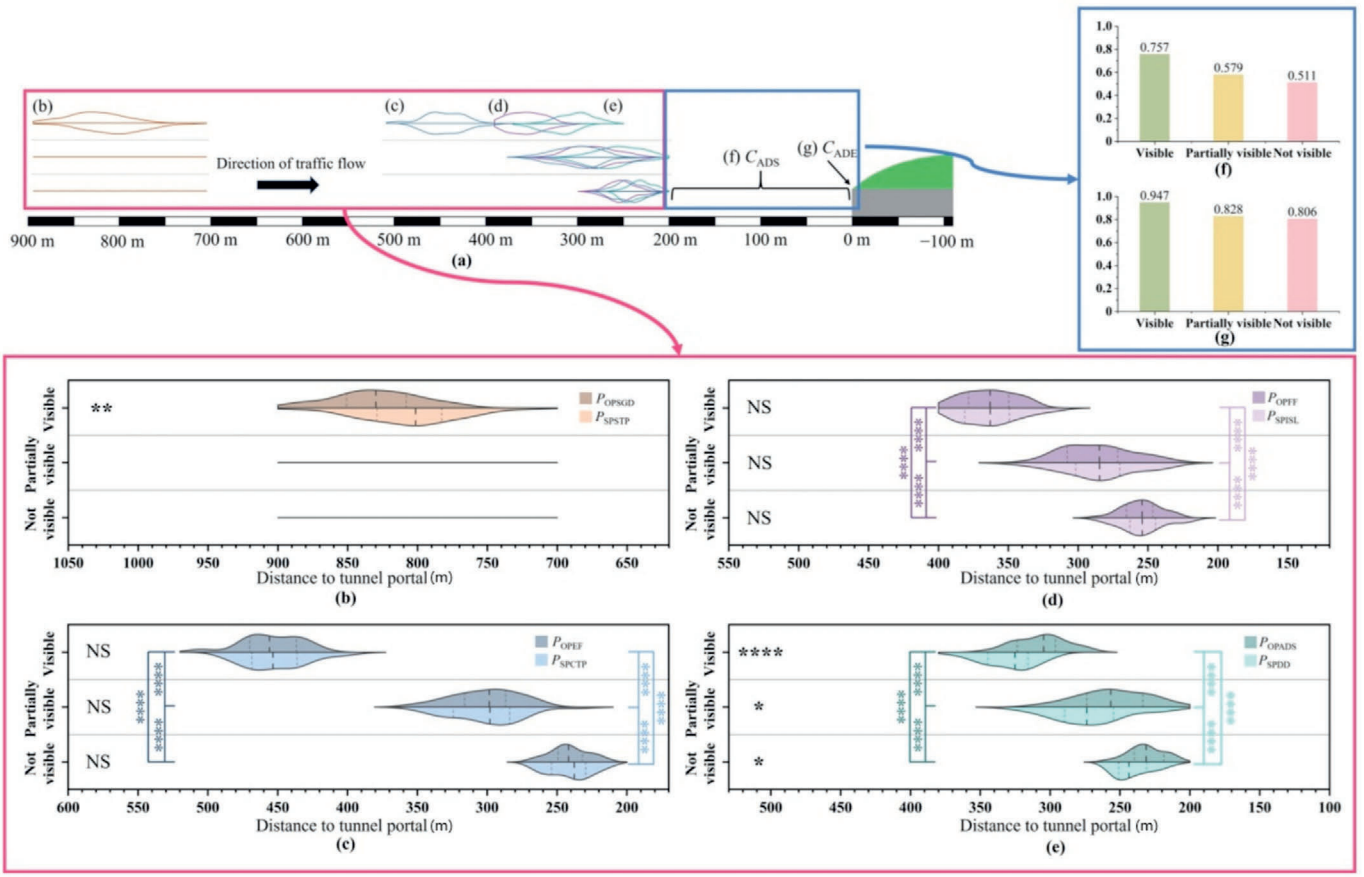

Fig. 5. Distribution of indicators for behavioral and cognitive chains, and safety and effectiveness coefficients of active deceleration behavior, under different visibility conditions in the tunnel approach zone. (a) Spatial overview of the evaluated indicators, (b) P_{OPSGD} & P_{SPSTP}, (c) P_{OPEF} & P_{SPCTP}, (d) P_{OPFF} & P_{SPISL}, (e) P_{OPSAD} & P_{SPDD}, (f) C_{ADS}, and (g) C_{ADE}.

(4) A consistent decision–action lag was evident in the deceleration process.

   (a) Both the decision point (P_{SPDD}) and the action point (P_{OPSAD}) shifted significantly closer to the portal as visibility worsened (P_{SPDD}: 329.54 m → 271.00 m → 240.28 m; P_{OPSAD}: 306.54 m → 254.66 m → 231.22 m), maintaining the order: visible ≫ partially visible > not visible. This indicates that drivers postpone both their deceleration decisions and execution under restricted sight conditions.
   (b) Across all the visibility conditions, the driver's intention to decelerate (P_{SPDD}) preceded the actual onset of active deceleration (P_{OPSAD}). For example, under visible conditions, P_{SPDD} occurred at 329.54 m while P_{OPSAD} followed at 306.54 m, confirming that active deceleration is a decision based maneuver.
   (c) Notably, the spatial gap between decision and action, the decision–action lag, varies with visibility. It was the largest under visible conditions (23.00 m), intermediate under partially visible conditions (16.33 m), and smallest under not visible conditions (9.06 m). Consequently, better sight distance provides greater temporal flexibility between the formation of deceleration intention and its physical execution.

(5) SSD designs degraded the safety and compliance of deceleration maneuvers.

Relative to the DSD-compliant baseline ($C_{ADS} = 0.76$, $C_{ADE} = 0.95$), SSD compliance reduced the active deceleration safety coefficient by 23.7% (partially visible) and 32.9% (not visible). The speed limit compliance (C_{ADE}) decreased by 12.6% and 14.7%, respectively. The fact that both SSD-compliant scenarios yielded similarly degraded safety (C_{ADS}) and compliance (C_{ADE}) outcomes serves as key evidence for the inadequacy of the standard in ensuring operational safety within TAZs.

4.2 Cognitive-behavioral workload in limited sight distance

4.2.1 Indicators about cognitive-behavioral workload

The operational and cognitive loads assessed in this section were derived from the spatiotemporal positions of the

key driving behaviors and cognitive nodes, which were obtained from the real-vehicle and subjective perception experiments detailed in Section 3.4. The data collection procedure and specific measures were as follows.

(1) Data source and primary measures

Operational load was quantified using the spatial positions of three key driving behavior nodes: P_{OPEF}, P_{OPFF}, and P_{OPSAD}. Cognitive load was quantified using the spatial positions of three key cognitive nodes, obtained from the subjective perception experiment: P_{SPCTP}, P_{SPISL}, and P_{SPDD}.

(2) Quantifying load via spatiotemporal compression

The standard Jaccard similarity coefficient (J) is a well-established metric used to compare the similarity and diversity of sample sets. It is defined as the size of the intersection divided by the size of the union of two sets, and is expressed mathematically as given in Eq. (6):

$$J = \frac{|A \cap B|}{|A \cup B|}. \tag{6}$$

With an adequate sight distance, these nodes are spatially separated, which allows tasks to unfold sequentially with a low load. The limited sight distance compresses these nodes closer together, which increases task overlap and workload. To quantify this compression, we propose the coefficient of extended Jaccard similarity (C_{EJS}). In this study, "workload" refers to the need for drivers to complete a series of driving behaviors or cognitive processes within a very short spatial interval with overlapping actions and thoughts. This concept aligns with the Jaccard similarity coefficient's aim to measure overlap between sets. C_{EJS} is thus defined as given below (Eqs. (7)–(10)):

$$C_{EJS} = \frac{|D_1| + 2|D_2| + 3|D_3|}{|A \cup B \cup C|}, \tag{7}$$

$$D_1 = A \cup B \cup C - A \cap B - A \cap C - B \cap C + 2(A \cap B \cap C), \tag{8}$$

$$D_2 = A \cap B + A \cap C + B \cap C - 2(A \cap B \cap C), \tag{9}$$

$$D_3 = A \cap B \cap C, \tag{10}$$

where A, B, and C represent the interval between the maximum and minimum values of specific indicators; D_1 refers to the non-overlapping regions of A, B, and C; D_2 represents the pairwise intersections of A, B, and C; D_3 denotes the complete overlap among A, B, and C. Given that higher degrees of overlap indicate greater hurriedness, we assigned higher weights to D_2 and D_3 in the equations.

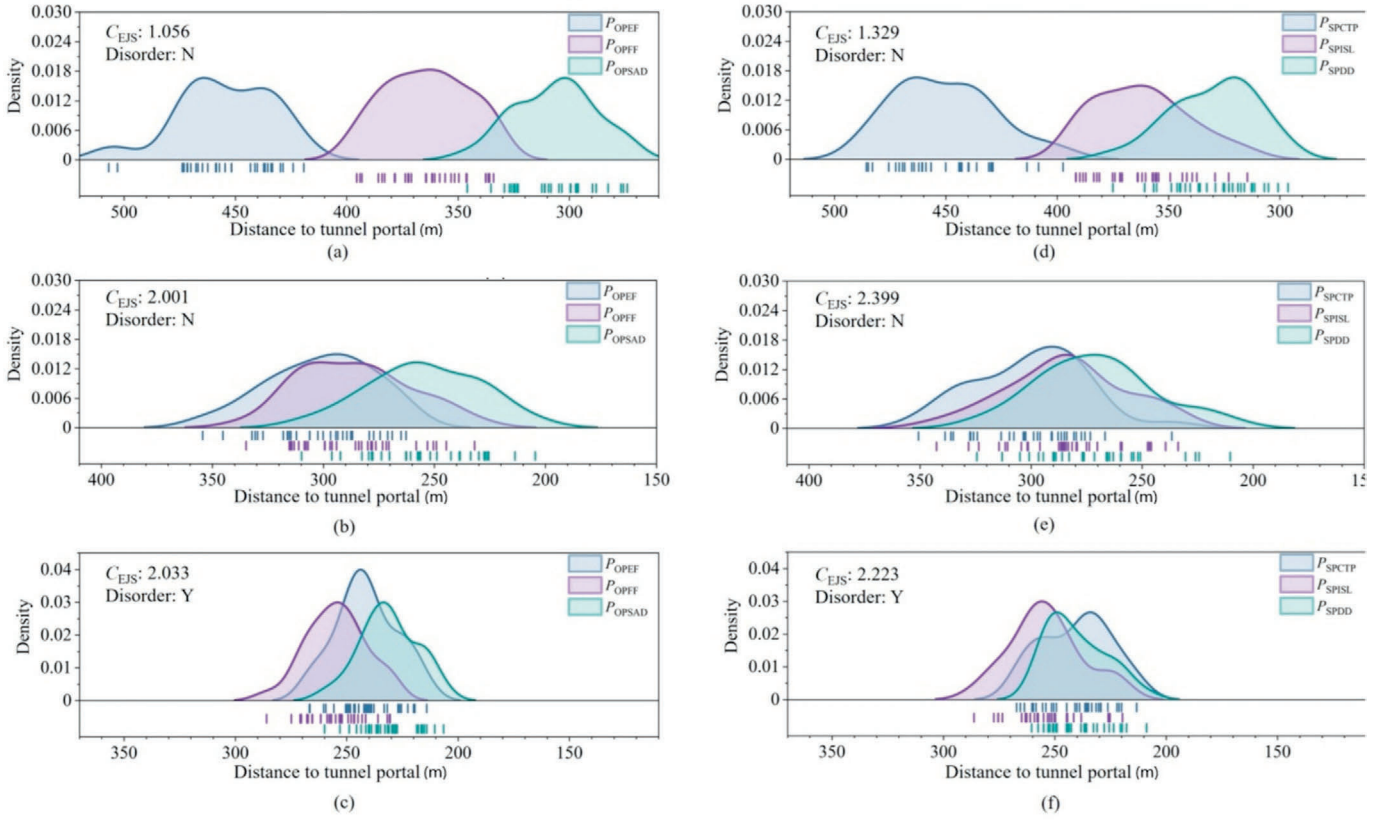

Fig. 6. Distribution of key driving behavior nodes and key driving cognitive nodes, their coefficient of extended Jaccard similarity (C_{EJS}), and presence of disorder under different visibility conditions in TAZs. (a) Driving behavior of visible condition, (b) driving behavior of partially visible condition, (c) driving behavior of not visible condition, (d) driving cognition of visible condition, (e) driving cognition of partially visible condition, and (f) driving cognition of not visible condition.

The value ranges from 1 (perfectly sequential, no overlap) to 3 (maximally compressed, complete overlap), with higher values indicating greater spatiotemporal compression, and thus a higher workload.

(3) Assessing disruption of the ordering of cognitive-behavioral processes

Beyond overall compression, severe sight restriction can disrupt the expected sequence of cognitive-behavioral processes. Therefore, we introduce a binary classification of the chain order.

(a) Orderly (N): The observed sequence of key nodes follows the expected, functionally logical order (e.g., confirming the presence of the tunnel confirmation before identifying the speed limit before forming an intention to decelerate).
(b) Disordered (Y): The observed sequence deviates from the expected order (e.g., speed limit identification occurs before tunnel confirmation), which indicates a breakdown in the normal cognitive-behavioral chain under extreme time pressure.

4.2.2 Analysis of cognitive-behavioral workload

Figure 6 depicts the distributions of key driving behavior nodes (P_{OPEF}, P_{OPFF}, and P_{OPSAD}) and key driving prediction nodes (P_{SPCTP}, P_{SPISL}, and P_{SPDD}) under varying visibility conditions, along with their C_{EJS} values and whether they are in a disordered state.

Under the visible condition, there was scarcely any overlap among the three key driving behavior nodes, and the C_{EJS} value was 1.056. In contrast, when the visibility was either partially visible or not visible, there was a large overlap among the three key driving behavior nodes. The C_{EJS} values were 2.001 and 2.033, respectively, which indicates that the degree of haste in driving behaviors nearly doubled.

Similarly, for the key driving prediction nodes under the visible condition, there was almost no overlap, and the C_{EJS} value was 1.329. When the level of visibility changed to partially visible or not visible, there was a significant overlap between them. The C_{EJS} values were 2.399 and 2.223, respectively, which suggests that the degree of haste in driving predictions also nearly doubled.

In particular, under the not visible condition, P_{OPFF} is disordered and occurs before P_{OPEF}. That is, drivers confirm the speed-limit requirements before they become aware of the tunnel ahead. The above analysis shows that, compared with the presence of a tunnel ahead, drivers are more concerned about the speed-limit requirements of the road section. When time is extremely tight, drivers will prioritize identifying the speed limit needs to avoid carrying out two behaviors simultaneously.

5 Discussion

5.1 Task analysis of driving scenarios and modified predictive processing model framework

The MPPM is applied as an explanatory framework to elucidate the mechanisms of risks revealed by the empirical data. The MPPM integrates and interprets the multidimensional metrics, including the key cognitive-behavioral nodes (P_{OPSGD}, P_{OPEF}, P_{OPFF}, P_{OPSAD}, P_{SPSTP}, P_{SPCTP}, P_{SPISL}, and P_{SPDD}) and performance coefficients (C_{ADS},

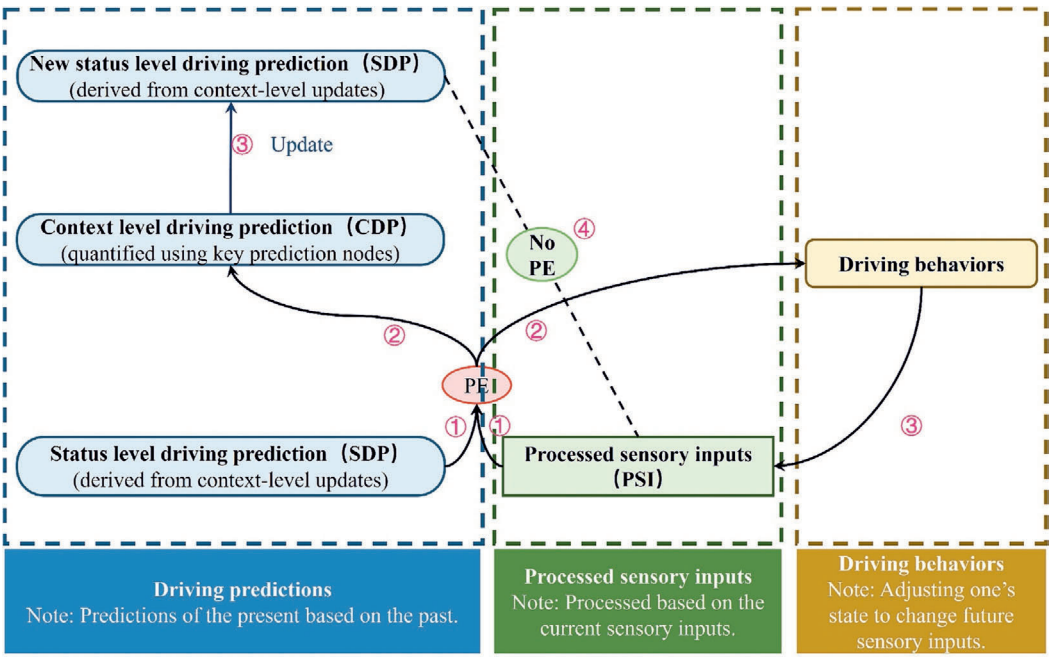

Fig. 7. Schematic diagram of the modified predictive processing model.

C_{ADE}), derived from the preceding TADS (Sections 3.3). In this integrated TADS–MPPM approach, TADS deconstructed the driving scenario into measurable, spatiotemporal components, answering "what" happens and "when". The MPPM then provides a model to synthesize these components by illustrating how disruptions in the flow of predictions, sensory input, and actions lead to the observed performance degradation and safety risks. The following section details the structure of the MPPM, which is subsequently used to visualize and contrast the cognitive-behavioral evolution under DSD and SSD conditions.

To quantify and visualize the dynamic interactions among driver expectations, tasks, behaviors, and sensory processing during the tunnel approach, we propose the MPPM, as illustrated in Fig. 7.

The MPPM structure comprises three hierarchical components. (1) Context level driving predictions (CDP): This quantifies high-level anticipatory states (e.g., deceleration intent) reflecting strategic decisions based on the roadway context. (2) Status level driving predictions (SDP): This component derives tactical expectations from the updated CDP states. (3) Processed sensory inputs (PSI): This repre-

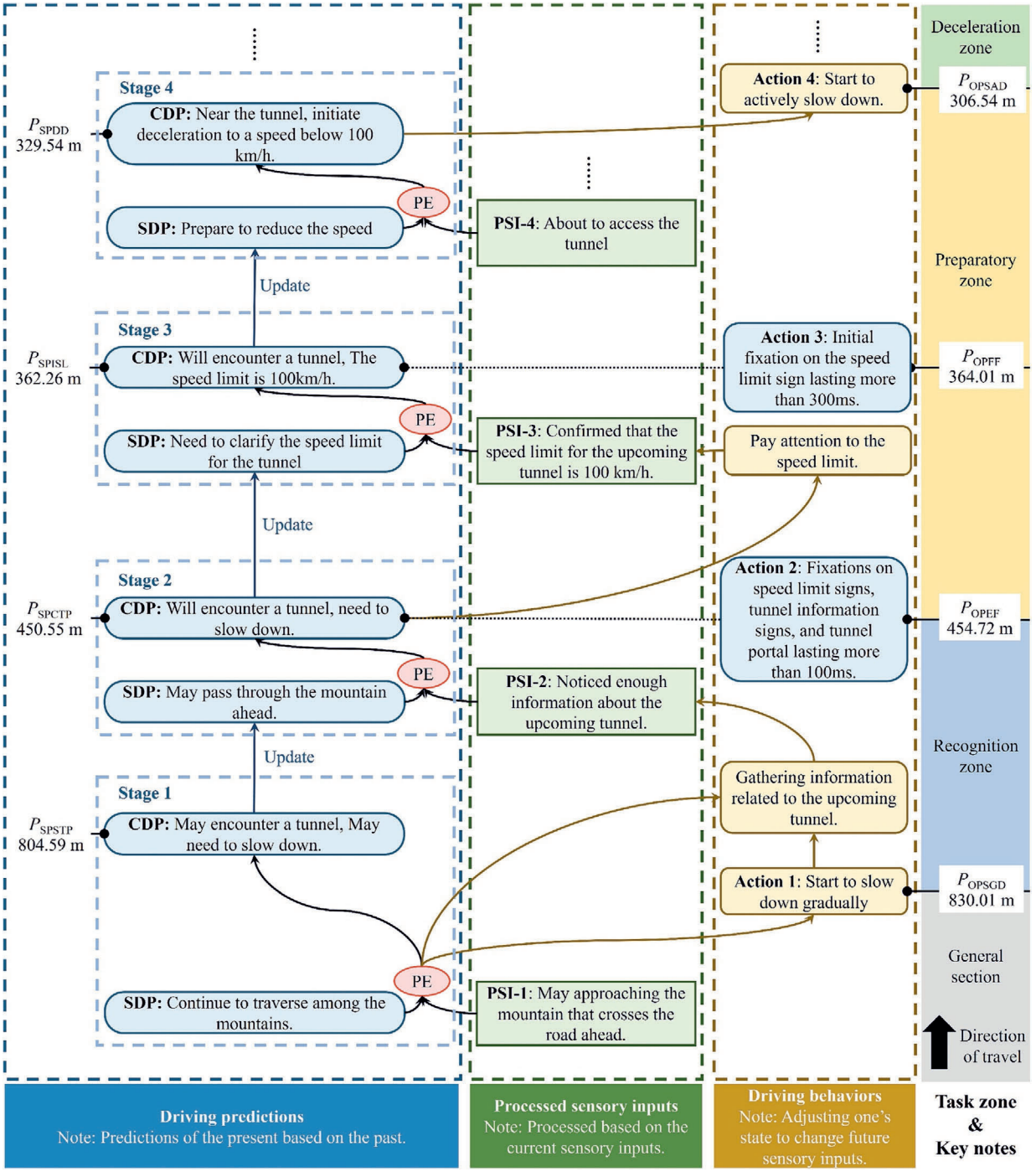

Fig. 8. Schematic of spatiotemporal evolution under DSD conditions.

sents abstracted environmental perceptions (e.g., visual cues and stress responses) after sensory filtering.

Environmental perturbations inducing discrepancies between PSI and SDP generate a prediction error (PE), triggering a dual adaptive response, which propagates upward to refine CDP and derivative SDP, while concurrently activating compensatory behaviors that modify PSI through adjusted vehicle kinematics; this closed-loop adaptation iterates until SDP–PSI realignment restores cognitive equilibrium.

5.2 Spatiotemporal evolution under DSD condition

Based on the MPPM and data analysis results of the key driving behavior nodes and key driving prediction nodes, the spatiotemporal evolution process of driving tasks, driving predictions, processed sensory inputs, and driving behaviors in freeway tunnel approach zones under standard conditions was constructed as shown in Fig. 8.

Several key pieces of information can be derived from Fig. 8:

(1) The incentives for gradual and active deceleration differ. Gradual deceleration stems directly from the PE between PSI and SDP. It is a direct result of environmental stimuli and is not a conscious operation by the driver. However, active deceleration originates from predictions at the context level. The driver first intends to decelerate and then proceeds to slow down.

(2) There was no significant difference between the objective position of ergodic fixation (P_{OPEF}) and the subjective position of confirming tunnel presence (P_{SPCTP}), and also no significant difference between the objective position of first fixation (P_{OPFF}) and the subjective position of identifying speed limit (P_{SPISL}). This indicates that predictions at the context level can be measured through eye-movement behaviors.

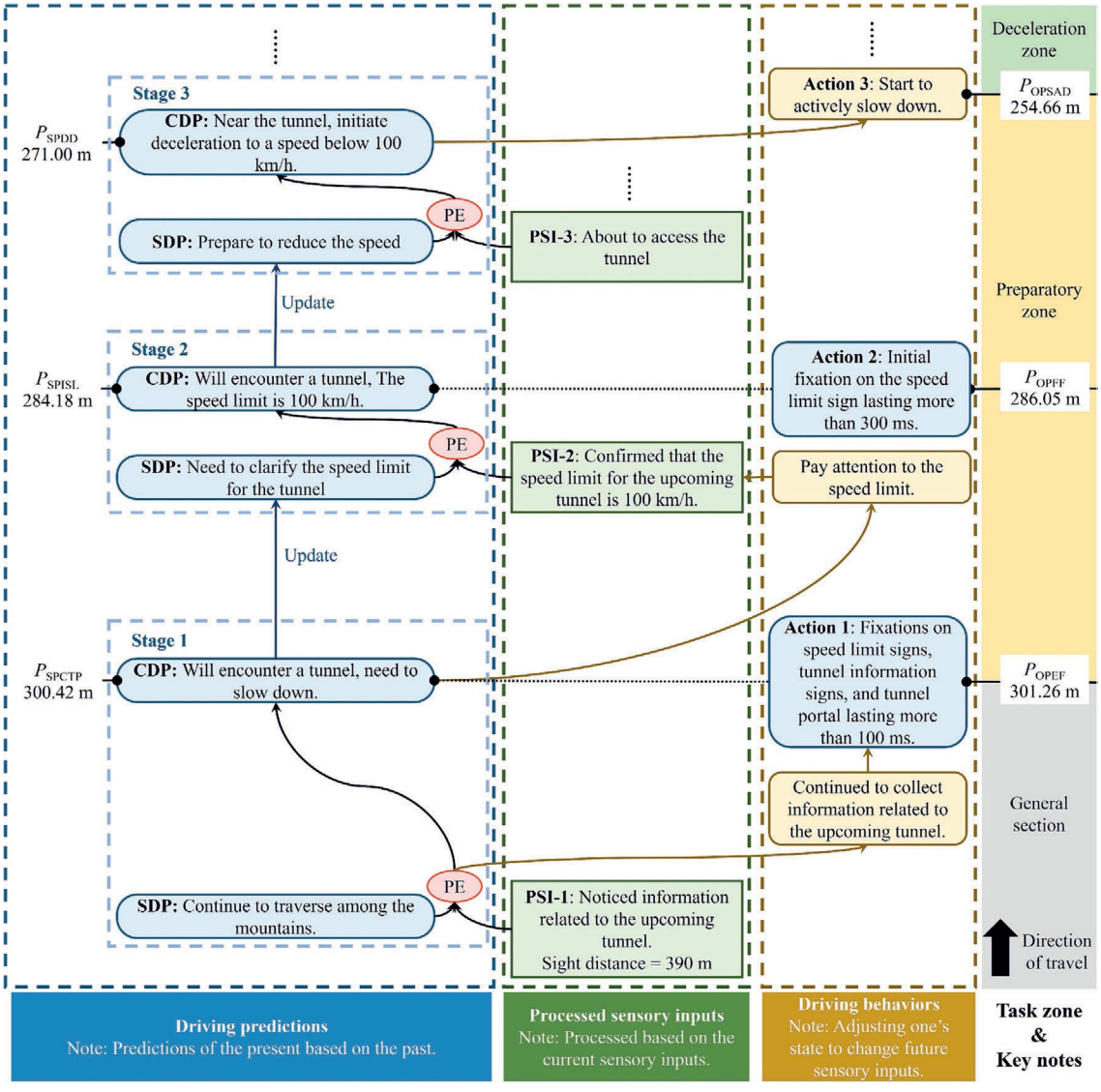

Fig. 9. Schematic of spatial–temporal evolution under SSD constraints.

In short, under the DSD condition, the driving predictions evolved gradually with consistently low prediction errors. This enables drivers to adjust their driving in a timely manner, resulting in good safety and effectiveness during the active deceleration phase. This was evidenced by the high values of C_{ADS} and C_{ADE}.

5.3 Spatiotemporal evolution under SSD constraints

Drivers must complete a series of interlinked cognitive and operational tasks within a limited space. Once external interferences emerge, it is highly likely to disrupt this delicate evolutionary process. The spatiotemporal evolution processes of driving tasks, driving predictions, processed sensory inputs, and driving behaviors in freeway TAZs under partially visible conditions, which can be regarded as external interferences, are depicted in Fig. 9.

By combining Fig. 9 with the data analysis results from the previous section, several key pieces of information can be obtained.

(1) When the visibility in the freeway tunnel approach zones is categorized as partially visible, drivers did not gradually decelerate when they were relatively far from the tunnel ahead (approximately 830.01 m) because the range of visibility was limited, and drivers could only see the information related to the tunnel ahead when they were 390 m away from it. As a result, the P_{OPEF}, P_{OPFF}, P_{OPSAD}, P_{SPCTP}, P_{SPISL}, and P_{SPDD} all lagged to varying degrees. It becomes difficult for drivers to timely detect the tunnel ahead, recognize the speed-limit signs, and decelerate.
(2) Drivers need to carry out a series of cognitive and operational tasks within a narrow space, and the intervals between various indicators are very short, leading to a state of hurry (C_{EJS} of key driving behavior nodes is $2.001 > 1.056$, and C_{EJS} of key driving cognitive nodes is $2.399 > 1.329$).
(3) Subsequently, to correct the prediction error, drivers might employ aggressive deceleration strategies, leading to lower C_{ADS} and C_{ADE}.
(4) When the visibility was poor, these situations deteriorated further, which ultimately led to a disorder in the cognitive and behavioral chains. Due to the extreme urgency of the situation, drivers were only able to prioritize the recognition of the most important information, namely the speed-limit signs, and then recognize other signs.

5.4 Contributions and limitations

Building upon the empirical evidence and the explanatory framework presented in this study, we first synthesize its primary theoretical and practical contributions. We then critically examine three key experimental limitations and explicitly describe how they necessitate specific modifications to the proposed design principles for TAZs. Finally, we outline a targeted research agenda aimed at transforming the validated qualitative principle into quantitative, context-sensitive design thresholds.

(1) Contributions

This research makes three primary contributions to the field. First, a novel TADS–MPPM framework was proposed, integrating task analysis with cognitive modeling to quantify the fine-grained spatiotemporal evolution of driving behavior in complex scenarios. Second, we have provided controlled experimental evidence that SSD compliance in TAZs is inadequate for safety by mechanistically linking SSD to compressed cognitive-behavioral chains, increased workload, and degraded maneuver quality. Third, and most significantly, a new design principle—to ensure safety redundancy, the critical visual information of a tunnel (portal, speed limit, and information signs) should be discernible at the DSD—was proposed and empirically validated.

(2) Limitations and implications for design principles

While the findings robustly demonstrate the insufficiency of SSD and the superiority of the DSD-based principle within our experimental context, four key limitations directly influence how this principle should be translated into generalizable design specifications.

(a) Passenger car focus & heavy vehicles. Our study used only passenger cars. The presence of heavy vehicles, with longer braking distances, greater inertia, and potentially different speed limits, fundamentally alters the safety equation (Saifizul et al., 2011). A DSD calculated for passenger cars may be inadequate for trucks, compressing their already critical deceleration zone. This implies that the proposed principle must evolve from a fixed DSD value to a performance-based or vehicle-class-adjusted sight distance criterion for TAZs. In practice, this could mean adopting the more demanding sight distance requirements of heavy vehicles as the governing standard for mixed-traffic corridors or designing truck-specific deceleration lanes where geometry permits.
(b) Absence of dynamic occlusion. Our free-flow experiments did not account for the dynamic visual occlusion caused by leading or adjacent vehicles, a prevalent condition in real-world traffic. Intermittent blockage of sight lines can delay a driver's detection of critical tunnel information beyond the delays measured under our static "partial visible" condition (Wang et al., 2024). Consequently, the principle of "discernibility at DSD" must be enhanced for robustness under occlusion. This refines the design guideline to incorporate redundancy and progressive disclosure, such as (i) positioning the first critical advance sign (e.g., tunnel warning) substantially upstream of

the nominal DSD to increase the likelihood of early detection, and (ii) implementing a multi-layer visual guidance system within the approach zone designed to the DSD standard to ensure continuous information availability even with intermittent sightline blockages (Bei et al., 2024a, 2024b).

(c) Single operational scenario. We tested a specific speed reduction (120 to 100 km/h). The kinetic energy to be dissipated, and thus the required reaction and deceleration distance, is sensitive to the speed differential (Ju et al., 2025). Generalizing our findings will require a functional relationship to be established between the approach speed, the tunnel speed limit, and the required decision sight distance. The core principle remains, but the specific DSD value becomes a variable to be calibrated across the common speed transition scenarios found in the road network.

(d) Specification of visual performance parameters. While this study provides a critical quantitative basis by validating the required distance (DSD), we did not specify the detailed visual performance parameters that ensure "discernibility" at that distance. To create fully actionable design guidelines, our findings must be complemented by future work that defines the requisite minimum size, luminance, contrast, and typography for signs and portals when viewed from the DSD under various environmental conditions (e.g., day, night, and rain). Establishing these linkable parameters between the geometric DSD and traffic control device standards remains a critical next step for practical implementation.

(3) Toward validated, context-sensitive visual thresholds

These limitations do not invalidate the core conclusion but rather chart the course for future research to transform the qualitative principle into quantitative, enforceable design standards. Future research should develop sight distance criteria that incorporate vehicle dynamics for mixed fleets, determine information detection probabilities under real traffic occlusion, create formulas linking required preview distance to approach/tunnel speed differentials, and define the minimum visual performance parameters (e.g., sign luminance, contrast, and size) necessary to guarantee the "discernibility" of critical tunnel elements at the adopted DSD. This will involve translating the human-factors-based DSD into companion specifications for traffic control devices and portal design.

6 Conclusions

This study demonstrates that applying only the SSD standard to TAZs fails to support their complex driving task demands. Through the lens of human factors, we have revealed the mechanism of safety risks to drivers on the road and proposed visibility conditions that ensure safety redundancy. Controlled real-vehicle experiments and subjective perception tests structured using the TADS–MPPM framework were conducted across three visibility conditions, including visible, partially visible, and not visible. Our key conclusions are summarized as follows.

(1) Limitations of SSD in TAZs

This study reveals that applying only SSD standards to TAZs disrupts the cognitive-behavioral sequence, which compromises the safety and compliance of the deceleration process. This compresses the perception–decision–action chain and forces drivers to execute multiple critical tasks within a drastically shortened window, which elevates operational risk. Conversely, ensuring that critical tunnel information is clearly discernible at the DSD restores this logic. It provides the necessary preview time and space to anticipate possible road scenarios and execute smooth maneuvers to reestablish the normal cognitive and behavioral order and thus enhance the margin of safety.

(2) Recommended visibility conditions for TAZs

To achieve the necessary safety redundancy, the visual design of TAZs must ensure that critical tunnel information, including speed limit signs, tunnel information boards, and the portal itself, is discernible at the DSD. For the operational scenario tested in this study (a design speed of 120 km/h on the approach, which requires deceleration for a highway tunnel), the required DSD is 415 m upstream of the portal. For other design speeds or traffic conditions, the corresponding DSD values can be obtained from established standards such as A Policy on Geometric Design of Highways and Streets (AASHTO, 2018).

(3) Contributions and limitations

This study makes three key contributions: (1) proposing the TADS–MPPM framework to quantify the evolution of cognition and behavior, (2) providing empirical evidence that SSD alone is insufficient in TAZs, and (3) validating DSD as the necessary sight distance standard to ensure safety redundancy. While these findings are constrained by the focus on passenger cars, free-flow conditions, and a single speed scenario, which limits their immediate generalization, they do establish a critical foundation for further investigation based on human factors. Future research can translate this principle into validated, context-sensitive design thresholds for mixed traffic and real-world conditions.

Data availability

The data that support the findings of this study are available from the corresponding author upon reasonable request.

CRediT authorship contribution statement

Runzhao Bei: Writing – review & editing, Writing – original draft, Visualization, Validation, Supervision, Software, Resources, Project administration, Methodology, Investigation, Formal analysis, Data curation, Conceptualization. **Zijun Du:** Methodology, Investigation, Formal analysis, Data curation, Conceptualization. **Nengchao Lyu:** Supervision, Project administration, Methodology, Investigation, Funding acquisition, Formal analysis. **Zhigang Du:** Resources, Methodology, Investigation, Data curation, Conceptualization.

Declaration of competing interest

The authors declare that they have no known competing financial interests or personal relationships that could have appeared to influence the work reported in this paper.

Acknowledgement

This work is supported by the National Natural Science Foundation of China (Grant No. 52472366), the National Key Research and Development Program of China (Grant No. 2023YFB4302600), and the Hubei Provincial Natural Science Foundation (Grant No. 2024AFD408).

References

American Association of State Highway and Transportation Officials (2018). *A policy on geometric design of highways and streets* (7th edition). Washington: IHS Markit.

Amundsen, F. H., & Ranes, G. (2000). Studies on traffic accidents in Norwegian road tunnels. *Tunnelling and Underground Space Technology, 15*(1), 3–11.

Bei, R., Du, Z., Huang, T., Mei, J., He, S., & Zhang, X. (2024a). Analysis and regulation of driving behavior in the entrance zone of freeway tunnels: Implementation of visual guidance systems in China. *Accident Analysis & Prevention, 202*, 107600.

Bei, R., Du, Z., Lyu, N., Yu, L., & Yang, Y. (2025). Exploring the mechanism for increased risk in freeway tunnel approach zones: A perspective on temporal-spatial evolution of driving predictions, tasks, and behaviors. *Accident Analysis & Prevention, 211*.

Bei, R., Wan, H., Du, Z., Huang, T., Han, L., & Mei, J. (2024b). Analysis and adjustment of vehicle trajectories in the entrance area of freeway tunnels: From the perspective of visual guiding system. *Promet-Traffic & Transportation, 36*(4), 639–653.

Calvi, A., De Blasiis, M. R., & Guattari, C. (2012). An Empirical Study of the Effects of Road Tunnel on Driving Performance. *Siiv-5th Internationsl Congress - Sustainbility of Road Infrastructures.*

Dou, S., Shen, Y., & Zhu, H. (2023). *Fuzzy-based multi-criteria humanistic assessment system for city tunnels: From methodology to application*. Tunnelling and Underground Space Technology (pp. 134).

Du, Z., Zheng, Z., Zheng, M., Ran, B., & Zhao, X. (2014). Drivers' visual comfort at highway tunnel portals: A quantitative analysis based on visual oscillation. *Transportation Research Part D: Transport and Environment, 31*, 37–47.

Fang, Y., Zhou, J., Hu, H., Hao, Y., Xiao, D., & Li, S. (2022). Combination layout of traffic signs and markings of expressway tunnel entrance sections: A driving simulator study. *Sustainability (Switzerland), 14*(6).

Feng, S., Kan, D., Zhou, L., Liu, X., Du, C., & Mao, W. (2025). Experimental study on effect of pavement background on obstacle visibility in LED lighting environment of road tunnel. *Underground Space, 22*, 124–136.

Han, L., & Du, Z. (2025). Unraveling the complex interplay between curved tunnels and drivers' physiological responses: An HRV perspective. *Transportation Research Part F-Traffic Psychology and Behaviour, 108*, 39–53.

Han, L., Du, Z., He, S., & Wang, S. (2024a). An empirical investigation of driver's eye-catching effect in the entrance zone of freeway tunnels: A naturalistic driving experiment. *Transportation Research Part F: Traffic Psychology and Behaviour, 101*, 92–110.

Han, L., Du, Z., & Ma, A. (2024b). Evaluation of traffic signs information volume at highway tunnel entrance zone based on the visual sample entropy of novice and experienced drivers. *Traffic Injury Prevention*.

He, S., Du, Z., Mei, J., & Han, L. (2025). Driving behavior inertia in urban tunnel diverging areas: New findings based on task-switching perspective. *Transportation Research Part F-Traffic Psychology and Behaviour, 109*, 1007–1023.

He, S., Liang, B., Pan, G., Wang, F., & Cui, L. (2017). Influence of dynamic highway tunnel lighting environment on driving safety based on eye movement parameters of the driver. *Tunnelling and Underground Space Technology, 67*, 52–60.

Hu, J., Sun, S., & Wang, R. (2022). Research on the influence of light source characteristics on traffic visual distance in foggy areas at night. *Building and Environment, 212*, 108818.

Hu, J. B., Zhang, X. Q., & Guo, D. (2016). Research on the tunnel entrance night light environment of highway tunnel based on visual safety. *Transaction of Beijing Institute of Technology, 36*(5), 487–490, 497 (in Chinese).

Hu, Y., Liu, H., & Zhu, T. (2019). Influence of spatial visual conditions in tunnel on driver behavior: Considering the route familiarity of drivers. *Advances in Mechanical Engineering, 11*(5).

Ju, Y., Ye, S., Chen, T., Xing, G., & Chen, F. (2025). How do drivers manage speed at tunnel entrances? Insights from uncorrelated grouped random parameters duration models for model invalidation and performance recovery times. *Analytic Methods in Accident Research, 45*.

Koustanaï, A., Boloix, E., Van Elslande, P., & Bastien, C. (2008). Formation of expectations while driving: Influence of the possibility and the necessity to anticipate on the ability to identify danger. *Transportation Research Part F: Traffic Psychology and Behaviour, 11* (2), 147–157.

Ling, J., Li, X., Shen, Y., Chen, C., Yan, Z., Zhu, H., & Li, H. (2025). Human centric VR system development supporting fire emergency evacuation: A novel knowledge-data dual driven approach. *Expert Systems with Applications, 273*.

Liu, H., Ding, G., Zhao, W., Wang, H., Liu, K., & Shi, L. (2011). Variation of drivers' visual features in long-tunnel entrance section on expressway. *Journal of Transportation Safety and Security, 3*(1), 27–37.

Liu, T., Zhu, H., Shen, Y., Xu, L., & Feng, S. (2025). Impact of tunnel lighting on driver perception and safety in foggy conditions. *Building and Environment, 285*, 113540.

Ma, Z., Chien, S. I. J., Dong, C., Hu, D., & Xu, T. (2016). Exploring factors affecting injury severity of crashes in freeway tunnels. *Tunnelling and Underground Space Technology, 59*, 100–104.

Ministry of Transport of the People's Republic of China. (2014). *Guidelines for Design of Lighting of Highway Tunnels* (JTG/T D70/2–02—2014). Beijing: China Communications Press (in Chinese).

Ministry of Transport of the People's Republic of China. (2017). *Design Specification for Highway Alignment* (JTG D20—2017). Beijing, China: China Communications Press (in Chinese).

Ministry of Transport of the People's Republic of China. (2025). *Traffic signs and markings—Part 3: Traffic markings* (GB 5768.3—2025). Beijing: China Communications Press (in Chinese).

Muhrer, E., & Vollrath, M. (2010). Expectations while car following-the consequences for driving behaviour in a simulated driving task. *Accident Analysis and Prevention, 42*(6), 2158–2164.

Pervez, A., Huang, H., Han, C., Wang, J., & Li, Y. (2020). Revisiting freeway single tunnel crash characteristics analysis: A six-zone analytic approach. *Accident Analysis and Prevention, 142*.

Pervez, A., Lee, J., & Huang, H. (2022). Exploring factors affecting the injury severity of freeway tunnel crashes: A random parameters approach with heterogeneity in means and variances. *Accident Analysis and Prevention, 178*.

Saifizul, A. A., Yamanaka, H., & Karim, M. R. (2011). Empirical analysis of gross vehicle weight and free flow speed and consideration on its relation with differential speed limit. *Accident Analysis and Prevention, 43*(3), 1068–1073.

Shao, X., Chen, F., Ma, X., & Pan, X. (2022). The impact of lighting and longitudinal slope on driver behaviour in underwater tunnels: A simulator study. *Tunnelling and Underground Space Technology, 122*.

Wang, X., Azati, Y., Quddus, M., Cai, B., & Zhang, X. (2024). Statistical Analysis of Traffic Crashes on Mountainous Freeway Tunnel Sections. *Transportation Research Record, 2678*(2), 1–10.

Wang, X., Liu, S., Cai, B., Hurwitz, D., Guo, Q., & Wang, X. (2023). Sample size study of driving simulator experiment for freeway design safety evaluations. *Transportation Research Record, 2677*(6), 73–92.

Wang, X., Zhu, M., & Chen, M. (2016a). Impacts of situational urgency on drivers' collision avoidance behaviors. *Journal of Tongji University (Natural Science Edition), 44*(6), 0876–0883.

Wang, Y. G., Wang, L. J., Wang, C., & Zhao, Y. D. (2016b). How eye movement and driving performance vary before, during, and after entering a long expressway tunnel: considering the differences of novice and experienced drivers under daytime and nighttime conditions. *SpringerPlus* (pp. 5).

Wickens, C. D. (2008). Multiple resources and mental workload. *Human Factors, 50*(3), 449–455.

Xu, L., Zhu, H., Shen, Y., Ling, J., & Feng, S. (2025a). Lighting environment design evaluation with digital workflow: A life cycle framework for integrating carbon and cost reduction strategies in tunnels. *Tunnelling and Underground Space Technology, 157*, 106363.

Xu, L., Zhu, H., Shen, Y., Liu, T., Ling, J., & Feng, S. (2025b). VR-based evaluation of fog-adaptive tunnel lighting and navigation aids on collision risk mitigation. *Advanced Engineering Informatics, 68*, 103777.

Yan, G., Wang, M., Qin, P., Yan, T., Bao, Y., & Wang, X. (2022). Comparative study on drivers' eye movement characteristics and psycho-physiological reactions at tunnel entrances in plain and high-altitude areas: A pilot study. *Tunnelling and Underground Space Technology, 122*.

Yang, Y., Du, Z., Alonso, F., Faus, M., & He, S. (2024). Why frequent traffic accidents at highway tunnel exit? – An experimental analysis of the slack effect. *Tunnelling and Underground Space Technology, 152*.

Yang, Y., Du, Z., Alonso, F., Faus, M., & Wan, H. (2025). Traffic safety improvement method for highway tunnel entrances based on linear guiding – An engineering practice from China. *Tunnelling and Underground Space Technology, 156*.

Zhang, J., Zhao, X., Li, H., Qi, J., & Xing, G. (2023). Evaluation of the Connected Vehicle Environment Effectiveness at Tunnel Entrance. *IEEE Transactions on Intelligent Transportation Systems, 24*(11), 11699–11709.

Zhang, Y., Yan, Z., Zhu, H., Shen, Y., Guo, Q., & Guo, Q. (2019). Experimental investigation of pedestrian evacuation using an extra-long steep-slope evacuation path in a high altitude tunnel fire. *Sustainable Cities and Society, 46*.

Zhu, T., Wang, C., Yang, C., & Zhao, R. (2020). Evaluation of effectiveness of speed reduction markings on driving speed in highway tunnel entrance and exit areas. *Promet - Traffic and Transportation, 32*(1), 141–152.